

MOMENTUM AND HEAT TRANSPORT INSIDE AND AROUND A CYLINDRICAL CAVITY IN CROSS FLOW

G. LYDON¹ & H. STAPOUNTZIS²

¹*Informatics Research Unit for Sustainable Engrg., Dept. of Civil Engrg.,
Univ. College Cork, Ireland, E-mail: glydon@mie.uth.gr*

²*Lab. of Fluid Mechanics & Turbomachinery, Dept. of Mechanical & Industrial Engineering,
University of Thessaly, Pedion Areos, 38334 Volos, Greece,
Tel.: +30 421 74109, Fax: +30 421 74052, E-mail: erikos@mie.uth.gr*

ABSTRACT

This paper deals with the transport of momentum and heat inside and around a cavity exposed to a boundary layer type cross flow. A cylindrical tube rests on a flat surface over which a turbulent boundary layer is developed. The cavity is formed by the cylinder side wall and a disk of adjustable height, parallel to the flat surface. The disk acts as a continuous source of heat. Quantities of interest are the velocity and temperature fields inside and in the wake of the cylinder. These quantities were measured in a wind tunnel and calculated using FLUENT 5.5 for Reynolds number (based on cavity diameter)= 1.44×10^4 .

The numerical mesh which was generated using GAMBIT1.3, is just under 400,000 nodes in size. It is a Hexahedral mesh taking advantage of GAMBIT's Multi-Axis Cooper Algorithm. The mesh was constructed with a boundary layer section and has a symmetry plane in order to reduce the computational effort. The numerical analysis was performed using FLUENT with the standard $k-\epsilon$ turbulence model together with the Reynolds-Averaged Navier-Stokes (RANS) equations. The velocity inlet was placed 30D upstream of the cylinder to allow for the development of the boundary layer. The boundary conditions were set using the hydraulic diameter and the turbulence intensity based on the experimental data. The velocity and temperature fields inside the cavity are influenced by buoyancy forces and cavity depth, the average Nusselt number being greater for the flush mounted heated surface and increasing with Re number. In the wake of the cavity, certain averaged temperature quantities like the maximum mean temperature and the maximum rms temperature exhibit a power law behaviour and are little affected by the cavity depth. Comparison of the experimental and computational results for mean velocity profiles upstream, downstream and at the cavity show good agreement. The rms velocities are also in good agreement except for the zone inside the cavity. In this location the computational values are greater than the experimental.

1. INTRODUCTION

Heat and mass transfer in cavities and enclosures has been the subject of increased. Such flows occur in many technological and industrial applications, either by design or circumstance, like in notches in turbine flow passages and combustion chambers, in spaces between heated electronic components, aircraft brake housing systems, buildings and solar thermal receiver systems. There are also environmental types of flows which fall into this category, namely those related to oil tank fires and pollutant transport in street canyons. Quite often, as in the present work, the heated, generally three dimensional, surfaces are partially or wholly exposed to an external forced flow. The study of heat transfer is then additionally complicated by possible boundary layer separation and reattachment inside and around the cavity, streamline curvature, formation of horseshoe vortices and recirculation.

Burggraf (1965), studied the effect of upstream boundary layer thickness on the mean velocity distribution of the separation streamline over rectangular surface cavities of different aspect ratios (length/depth). His model, developed for high Reynolds numbers and assuming a

single rotational core, indicates a decrease in this mean velocity with increasing boundary layer thickness and cavity depth. Assuming constant wall temperatures, the heat flux was higher on the downstream portion of the cavity. However, as Koseff et al., (1990) point out, two dimensions may not be sufficient for the computation of otherwise two dimensional (i.e. long span) cavities due to the existence of unsteady three dimensional structures. It is generally found, e.g. Richards et al., (1987), that the average Nusselt number of heated two dimensional rectangular cavities increases with the Reynolds number and the width to depth cavity ratio. At a range of low Reynolds numbers however, and when an array of sources is placed in the streamwise direction, e.g. Mahaney et al., (1990), the Nusselt number may actually decrease, due to the thermal instabilities and buoyancy driven secondary flow. Certainly the Nusselt number depends strongly on the Rayleigh or Grashof number in this regime. Most of the related research work deals with simple rectangular or "notched" type cavity geometries, Hoydysh & Dabberdt (1988). In the present paper the momentum and heat transport from a bottom-heated cylindrical cavity was investigated. The flow field is that around a hollow axisymmetric circular cavity in a cross flow and resting on a solid boundary, as shown in Fig. 1. The purpose is to study the mixing of the heated entrained fluid inside the cavity and in its wake, both numerically using FLUENT and experimentally in a wind tunnel. Results of the isothermal case (no heating) are presented in this paper.

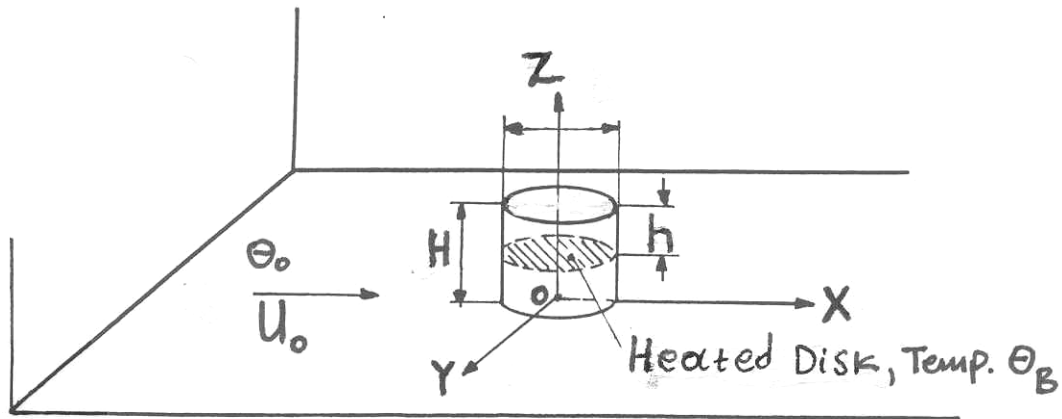


Figure 1: Layout of Circular Cavity in Cross Flow Resting on plane $z=0$.

2. COMPUTATIONAL MODEL

2.1. Model

The computational grid is based on the geometry of the wind tunnel. The geometry is rectangular (Fig. 2). The model has a velocity inlet on one end face and a pressure outlet on the other. The cylinder is located in the centre of the domain. A symmetry plane is used in order to reduce the number of nodes required. The flow is dominant in one direction therefore a block-structured mesh is used. This block structure gives the necessary control to adjust mesh spacing in various zones. The geometry dimensions of the model are as follows:

	Meters
x-direction (Direction of Flow)	2.3
y-direction	0.15
z-direction	0.30
Cylinder Height	0.054
Cylinder Radius External	0.027
Cylinder Radius Internal	0.024

Table 1: Model Dimensions.

The main difficulty encountered in building the grid, was the construction of the multi-blocks around the Cylinder and mapping together all other areas of interest consistently. The combining and splitting of faces technique facilitated this approach, by enabling a smooth transition of nodes between complex and regular areas, Fig. 3. GAMBIT's Cooper Algorithm was used to mesh the non-rectangular blocks.

The distance from the start of the floor mesh to the cylinder was adjusted in order to match the boundary layer development with the experimental data. A distance of approximately 20D was used. The x-velocity plots for the computational and experimental are in good agreement, which is due to the boundary layer mesh that was added to insure accurate development, Fig. 4. An inlet profile input could have been used to set up the boundary layer. This would have reduced the number of nodes. The spacing in the initial section is coarse, therefore the saving would not have been large. The mesh size is approximately 500,000 nodes with the following distribution:

Direction	Number of nodes
x-direction	270
y-direction	22
z-direction	80

Table 1.2 Mesh Size.

It was estimated that the overall average y^+ value would lie below 30 for all cases under investigation and associated boundary conditions. The boundary conditions were set as follows:

Description	Boundary Condition
Air Inlets	Velocity Inlet
Exhaust	Pressure Outlet
Walls	Non-slip Walls

Table 1.3 Boundary Conditions.

The model was within the acceptable accuracy when analysed by GAMBIT's *Examine Mesh Tool* for Equi-angle Skewness and Aspect Ratio.

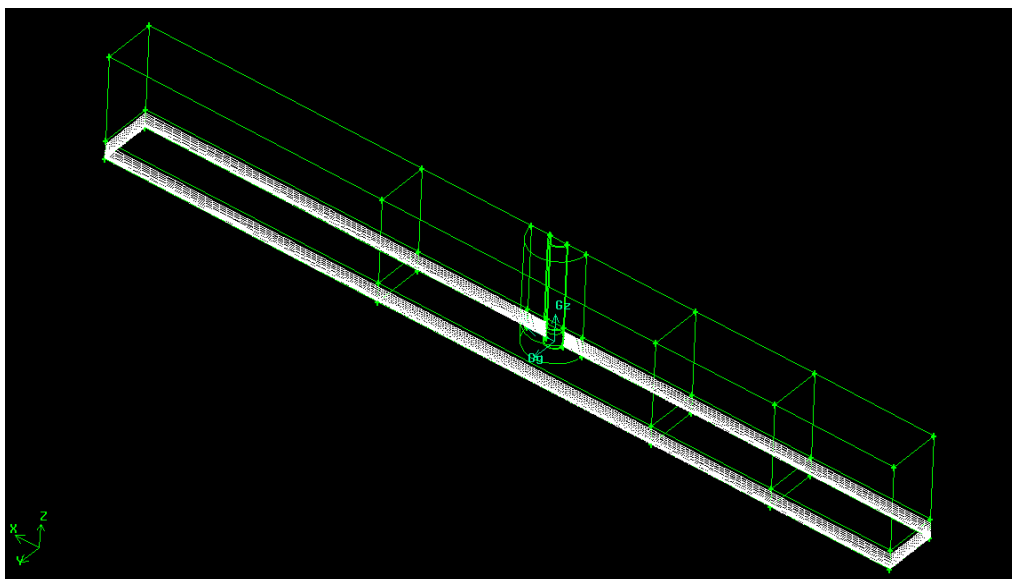


Figure 2: Flow Geometry.

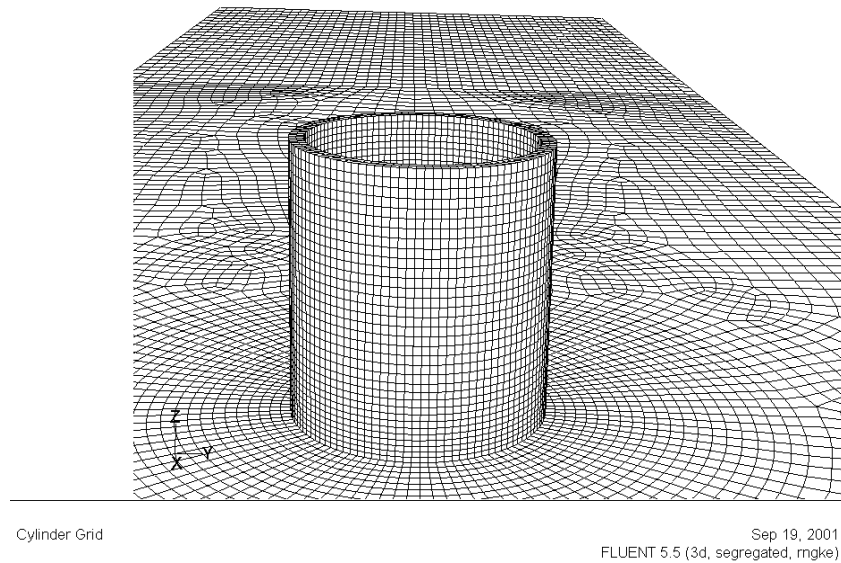


Figure 3: Surface Mesh.

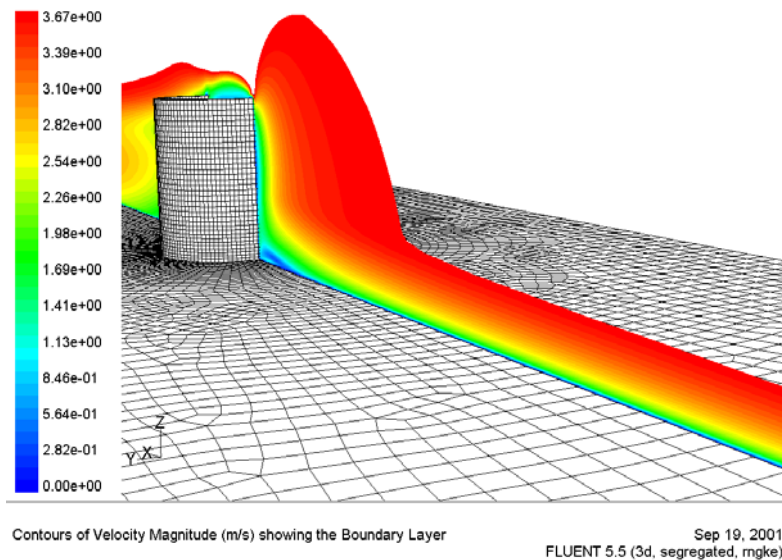


Figure 4: Upstream Boundary Layer Development.

2.2. FLUENT Settings

The numerical analysis was performed using FLUENT with the Standard $k-\epsilon$, RNG $k-\epsilon$ and the Reynolds Stress turbulence models. Due to the dominance of the flow in one direction the convergence was relatively fast. The $k-\epsilon$ models converged after approximately 160 iterations and the Reynolds Stress after 310 iterations. A convergence monitoring point was set up 1D downstream of the cylinder. The properties monitored at this point were x-velocity and turbulent intensity. The boundary conditions for the velocity inlet and pressure outlet were set using the hydraulic diameter and turbulent intensity. The initial velocity and turbulence intensity were estimated from experimental data.

3. FLUENT COMPUTATIONS AND COMPARISON WITH EXPERIMENT

The cavity diameter was $D=0.054\text{m}$, equal to its height H , the depth $h/H=0.25$, and the Reynolds number $Re=U_0D/\nu=1.44\times 10^4$. The computed external mean velocity U_0 and the boundary layer thickness δ at $10D$ upstream of the cavity were matched to these obtained from the experiments. The freestream turbulence was in both cases 0.5%. Fig. 5 shows the

vertical computed streamwise velocity distributions for various streamwise positions, upstream, inside and in the wake of the cavity. No heating was applied at this stage.

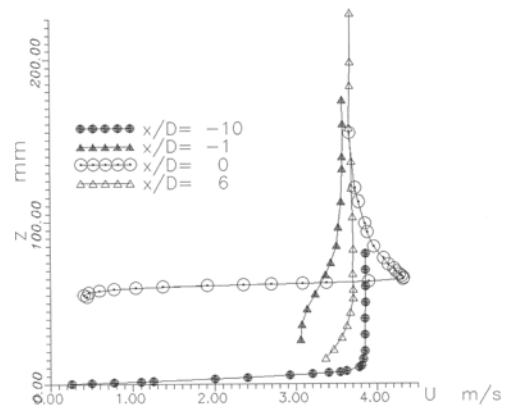
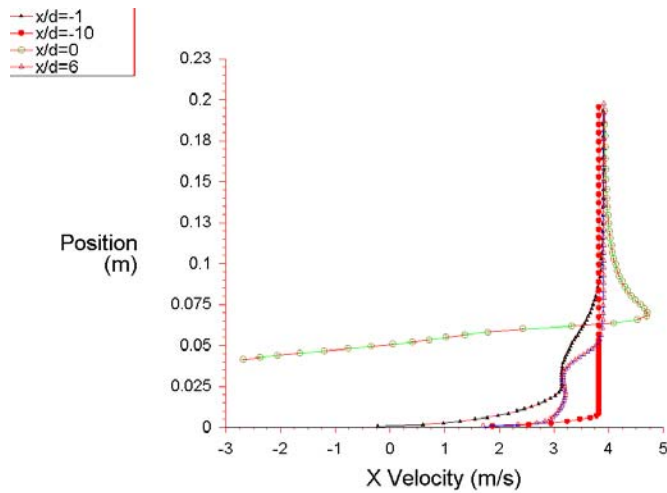
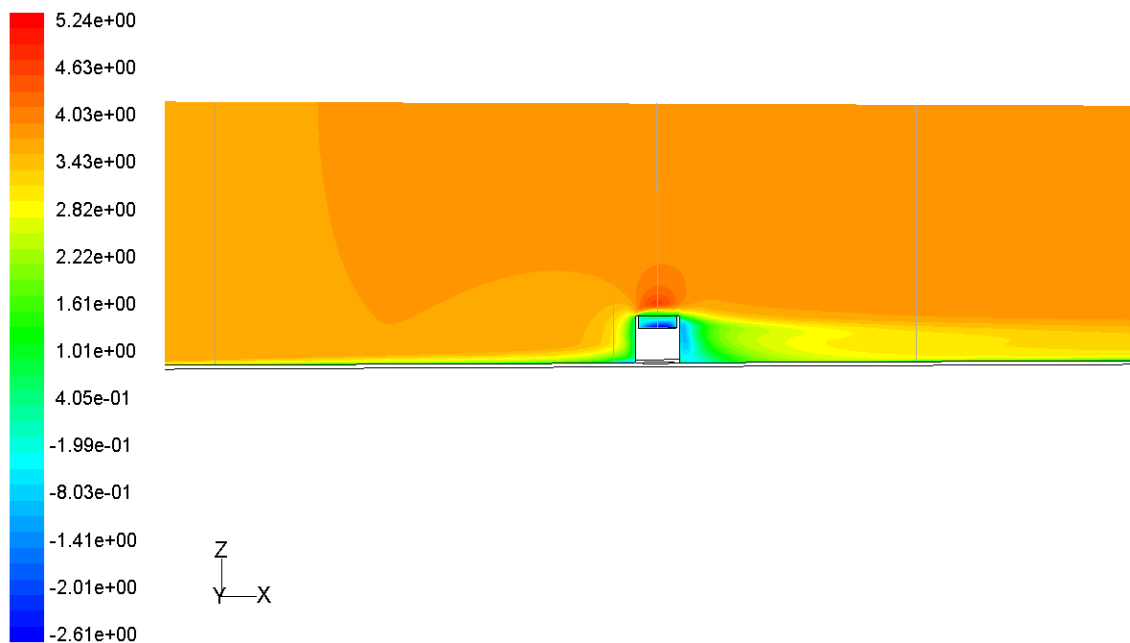


Figure 5: Computed Mean Streamwise (U_x) Velocity Profiles.

Figure 6: Experimental Mean Streamwise (U_x) Velocity Profiles.

It is observed that the computed and experimental velocity profiles at $x/D=-10$, are in good agreement for almost all z , although U_0 and δ were only matched at this streamwise position. One diameter upstream of the cavity, $x/D=-1$, the agreement is still good, improving at positions above the cavity height ($z/H>1$). Both the experiment and the computed values indicate a low velocity area just upstream of the cavity, signaling the stagnation region, Figs. 7, 8.



Contours of X Velocity (m/s)

Figure 7: Computed Magnitude of Streamwise Velocity,

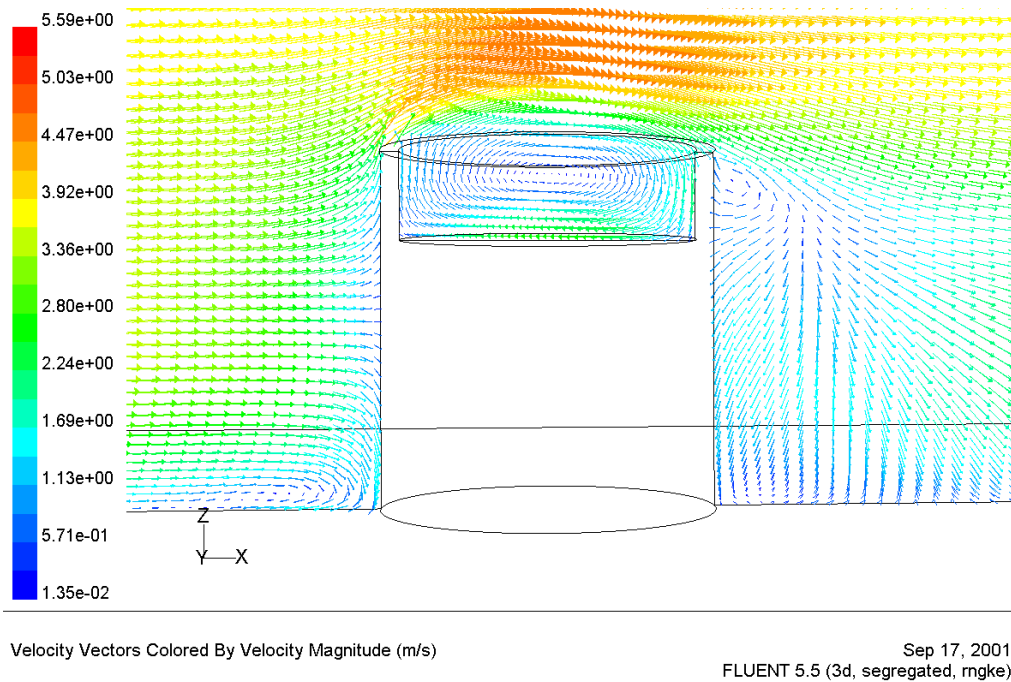


Figure 8: Computed Velocity Vectors.

The velocity was measured with a hot wire. For this reason, no confidence was put on data for $z/D < 0.5$, where flow visualization has indicated low velocities and a recirculation region. The usefulness of FLUENT is that it provides a picture of the flow down to the solid surface ($z=0$).

The velocity profiles at $x/D=0$, i.e. the center of the cavity, are very similar. The largest velocity magnitude appears at $z/D=1.2$, both in computations and experiment. This is also the area where the u velocity fluctuations are very big, reaching an rms level of 17% in the experiments. No measurements were taken inside the cavity ($z/D < 1$). FLUENT shows that negative velocities appear as soon as the top of the cavity is reached. The magnitude of the reverse velocity near the bottom of the cavity is of the order of the (positive) velocity close to the top, thus pointing to a vortex-type recirculation region, Fig. 9. This vortex is however much different than that realized in a two dimensional cavity, as the top view of Fig. 10 demonstrates.

The agreement between the experimental and computed values is fair in the wake region, $x/D = 6$. The experiment shows a gradual recovery to the free stream velocity as the distance from the floor increases, while FLUENT gives a more constant streamwise velocity magnitude over the height of the cavity, $z/D=1$ and then a rapid recovery. The experimental rms velocity exhibits a similar behavior, dropping from a value of 7% at $z/D=0.3$ to 2% at $z/D=10$ (height of cavity).

4. CONCLUSIONS

The computation of the flow in an axisymmetric cavity was accomplished using FLUENT. Mean velocity data are in good agreement to the experimental ones, but in some regions of the flow field the agreement was fair. More computational data will be available in future runs, where velocity fluctuations and temperature profiles will be compared to those obtained experimentally.

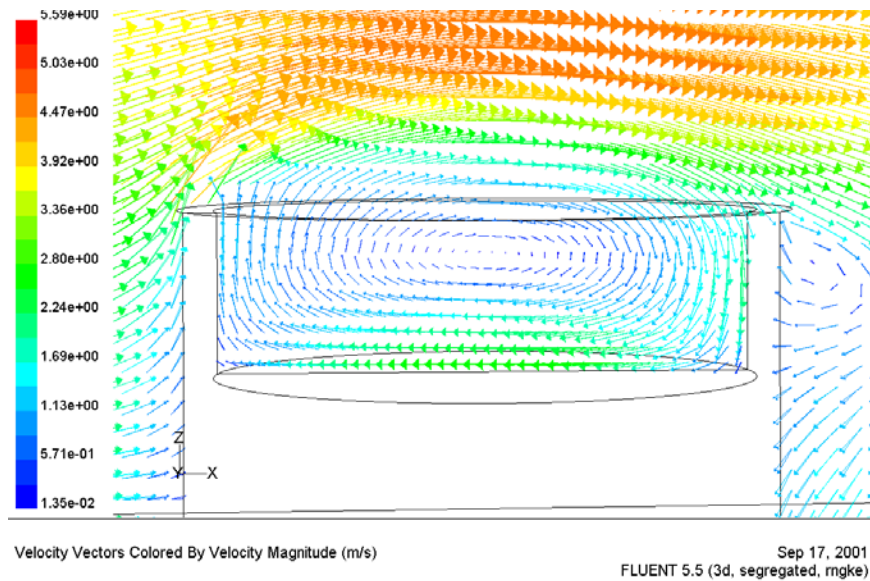


Figure 9: Computed Velocity Vectors Inside and Above Cavity.

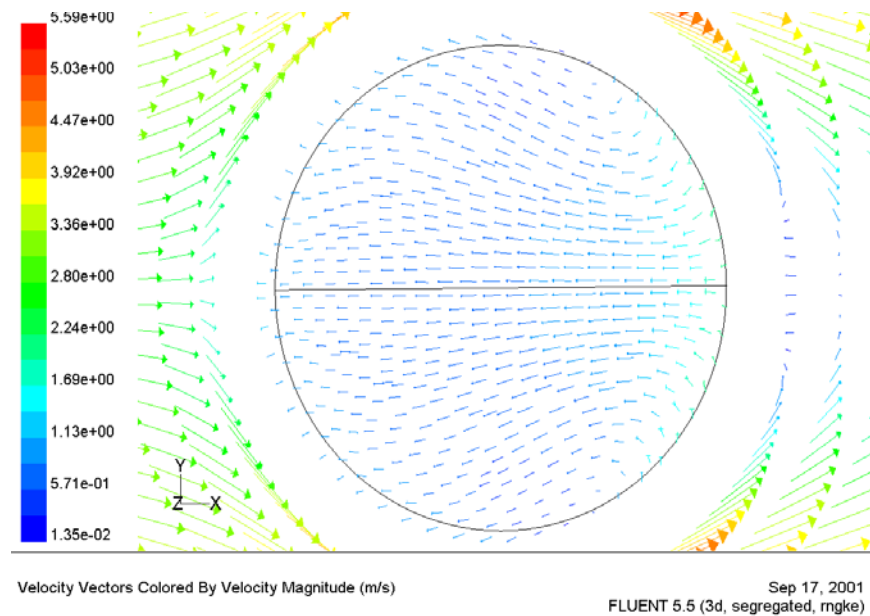


Figure 10: Velocity Vectors at $z/D=0.875$ Plane.

REFERENCES

- [1] Burggraf, O. R., (1965). "A model of steady separated flow in rectangular cavities at high Reynolds number", *Proc. Heat Transfer and Fluid Mech. Inst.*, Stanford Univ. Press, A.F. Charwat (Ed.), pp. 190–229.
- [2] Hoydysh, W. G., & Dabberdt, W. F., (1988). "Kinematics and dispersion characteristics of flows in asymmetric street canyons", *Atmosph. Environ.*, **22**(12), pp. 2677–2689.
- [3] Koseff, J. R., Prasad, A. K., Perng, C., & Street, R.L., (1990). "Complex cavities: Are two dimensions sufficient for computation?", *Phys. Fluids*, **A2**(4), pp. 619–622.
- [4] Richards, R. F., Young, M. F., & Haiad, J. C., (1987). "Turbulent forced convection heat transfer from a bottom heated open surface cavity", *Int. J. of Heat and Mass Transfer*, **30**(11), p. 2281.